



The histone deacetylase 1/GSK3/SHAGGY-like kinase 2/BRASSINAZOLE-RESISTANT 1 module controls lateral root formation in rice

Jiaqi Hou ¹, Xueke Zheng,¹ Ruifei Ren,¹ Qipeng Shi ,¹ Huangzhuo Xiao,¹ Zhenfei Chen,¹ Mengxia Yue,¹ Yequn Wu,¹ Haoli Hou¹ and Lijia Li ^{1,*†}

¹ State Key Laboratory of Hybrid Rice, College of Life Sciences, Wuhan University, Wuhan 430072, China

*Author for correspondence: ljli@whu.edu.cn

†Senior author.

J.H., R.R., Q.S., H.X., and X.Z. performed the experiments, Z.C., M.Y., Y.W., and H.H. performed part of data analysis. J.H. and L.L. designed research, analyzed data, and wrote the paper.

The author responsible for distribution of materials integral to the findings presented in this article in accordance with the policy described in the Instructions for Authors (<https://academic.oup.com/plphys/pages/general-instructions>) is: Lijia Li (ljli@whu.edu.cn).

Abstract

Lateral roots (LRs) are a main component of the root system of rice (*Oryza sativa*) that increases root surface area, enabling efficient absorption of water and nutrients. However, the molecular mechanism regulating LR formation in rice remains largely unknown. Here, we report that histone deacetylase 1 (OsHDAC1) positively regulates LR formation in rice. Rice *OsHDAC1* RNAi plants produced fewer LRs than wild-type plants, whereas plants overexpressing *OsHDAC1* exhibited increased LR proliferation by promoting LR primordia formation. Brassinosteroid treatment increased the LR number, as did mutation of *GSK3/SHAGGY-like kinase 2* (*OsGSK2*), whereas overexpression of *OsGSK2* decreased the LR number. Importantly, OsHDAC1 could directly interact with and deacetylate OsGSK2, inhibiting its activity. OsGSK2 deacetylation attenuated the interaction between OsGSK2 and BRASSINAZOLE-RESISTANT 1 (OsBZR1), leading to accumulation of OsBZR1. The overexpression of *OsBZR1* increased LR formation by regulating Auxin/IAA signaling genes. Taken together, the results indicate that OsHDAC1 regulates LR formation in rice by deactivating OsGSK2, thereby preventing degradation of OsBZR1, a positive regulator of LR primordia formation. Our findings suggest that OsHDAC1 is a breeding target in rice that can improve resource capture.

Introduction

The lateral root (LR) is a main component of the plant root system; its formation is controlled by an endogenous program and external environmental conditions (Malamy, 2005; Gifford et al., 2013; Yu et al., 2016). Understanding the regulation of LR formation is of great agronomic value because LR formation increases the absorbing surface for efficient water and nutrient uptake; it also provides better plant anchorage (Orman-Ligeza et al., 2013; Rogers and Benfey, 2015; Meng et al., 2019). Arabidopsis (*Arabidopsis thaliana*) is a

model dicot plant with a taproot system composed of an embryonic primary root and postembryonic LRs arising from the primary roots (Dubrovsky et al., 2000; Marhavý et al., 2016; Motte et al., 2019); rice (*Oryza sativa*) is a model monocot cereal, which forms a fibrous root system consisting of an embryonic primary root, several seminal roots, and the LRs generated from primary and seminal roots (Coudert et al., 2010; Yu et al., 2016). Arabidopsis LRs completely emerge from pericycle cells (Dubrovsky et al., 2000; Marhavý

et al., 2016; Motte et al., 2019). In contrast, the LRs in cereals are formed via division of the pericycle and endodermis cells (Coudert et al., 2010; Yu et al., 2016). Auxin is a key hormone that regulates LR formation; numerous components of auxin signaling pathways are involved in several stages of LR formation in Arabidopsis (Bhalerao et al., 2002; Lv et al., 2021; Singh et al., 2020). Other hormones have also been reported to regulate LR formation. For example, cytokinin and abscisic acid function as negative regulators of LR formation; brassinosteroid (BR) positively regulates LR formation, possibly by interacting with auxin-regulated genes in Arabidopsis (Fukaki and Tasaka, 2009; Jia et al., 2021). Most available information concerning the involvement of these hormones in LR formation is obtained from studies in Arabidopsis. Numerous auxin-related genes are involved in LR formation in cereals, such as auxin signaling transduction genes, auxin transport genes, and cell cycle-regulated genes (Malamy, 2005; Yu et al., 2015; Yamauchi et al., 2019; Mao et al., 2020). Little is known regarding the mechanisms by which BR and the components of BR signaling pathways affect LR formation in rice.

Histone deacetylases (HDACs) in plants can be classified into three types, two of which are identified according to their sequence similarity to three HDAC families in yeast: reduced potassium dependency 3 (*RPD3*)/histone deacetylase 1 (*HDA1*) and silent information regulator 2 (*Sir2*). The third type is a plant-specific class of HDACs, *HD2* (Pandey et al., 2002). HDACs have functions in plant growth and development, as well as responses to external and internal cues. *HDA19* (*AtRPD3A* or *AtHD1*) is involved in the ethylene and jasmonic acid signaling pathways in response to pathogens in Arabidopsis (Zhou et al., 2005). Arabidopsis *HDA6* (*AtRPD3B*) mediates heterochromatin silencing (To et al., 2011). *HDA101* is related to gene transcription in maize (Rossi et al., 2007). The overexpression of the *RPD3*-type HDAC gene *OsHDAC1* increases root growth in rice seedlings and alters rice architecture (Jang et al., 2003). The *HD2*-subfamily member *HDT701* negatively regulates rice innate immunity (Ding et al., 2012). HDACs regulate gene expression by removing the acetyl moieties from acetylated lysines of histones. However, many nonhistone proteins are acetylation targets of HDACs, which affect various cellular pathways (Narita et al., 2019). The acetylation of metabolic enzymes in response to extracellular nutrient flux directly affects enzyme activity or stability (Zhao et al., 2010). Reversible lysine acetylation is a modification of multiple nonhistone proteins in Arabidopsis (Wu et al., 2011). In Arabidopsis, *HDA6* interacts with and deacetylates BRASSINOSTEROID-INSENSITIVE 2 (*BIN2*) kinase to inhibit its activity, which may be related to energy status (Hao et al., 2016). Acetylated proteins are also implicated in the regulation of plant metabolic processes, such as photosynthesis and respiration (Shen et al., 2015). There are 17 HDAC genes in the rice genome (Hou et al., 2021), but the functions and underlying mechanisms of most *OsHDAC* genes are unclear.

In rice, several primary BR signaling components have been identified. *OsGSK2* encodes a GSK3/SHAGGY-like kinase that negatively regulates BR signaling and phosphorylates the transcription factor *OsBZR1*, leading to its proteasome-mediated degradation (Peng et al., 2008; Tong et al., 2012). Here, we report that *OsHDAC1* positively regulates LR formation by inducing LR primordia formation in rice. *OsHDAC1* functions to deacetylate and deactivate *OsGSK2*, preventing its interaction with *OsBZR1*. This results in the accumulation of *OsBZR1* to promote the expression of LR formation-related genes and LR initiation in rice. Our findings show that this *OsHDAC1*–*OsGSK2*–*OsBZR1* module mediates LR formation in rice.

Results

OsHDAC1 positively regulates LR development in rice

HDACs have important roles in various biological processes. In rice, there are 17 HDAC genes, 14 of which are the *RPD3/HDA1* type (Hou et al., 2021). Transcriptional changes in *RPD3/HDA1*-type deacetylase genes were first investigated to unravel the potential involvement of *OsHDACs* in rice growth and development. Analysis of the published RNA-seq data sets from rice (*O. sativa* L.) revealed that *OsHDAC1* transcripts were highly abundant in roots, leaves, seeds, young panicles, and shoot apical meristems (Supplemental Figure S1A). A quantitative real-time polymerase chain reaction (RT-qPCR) experiment confirmed the high abundance of *OsHDAC1* transcript in roots, leaves, and shoots (Supplemental Figure S1B). Phylogenetic analysis revealed that *OsHDAC1* exhibits 78.60% amino acid sequence similarity with the extensively studied Arabidopsis *HDA19* (Supplemental Figure S2, A and 2, B). The five key deacetylase sites for HDAC activity in *OsHDAC1* were highly conserved (Supplemental Figure S2C). Arabidopsis *HDA19* regulates many aspects of plant development and stress response (Chen et al., 2020), suggesting comparable roles for rice *OsHDAC1*.

To determine the subcellular localization of *OsHDAC1*, *OsHDAC1*–sGFP fusion proteins encoded by an HBT-sGFP vector were transiently expressed in rice protoplasts. *OsHDAC1* was detected in the nucleus and cytoplasm, implying roles in nuclear and cytoplasmic protein deacetylation (Supplemental Figure S3). To investigate the function of *OsHDAC1* in protein deacetylation and rice development, we produced RNA interference and gain-of-function transgenic plants. Transgenic rice plants overexpressing (OE) *OsHDAC1* were generated using a pCXUN vector that contained the *OsHDAC1* CDS fused to the HA tag under the control of the ubiquitin promoter (Supplemental Figure S4A). We obtained 10 OE lines with increased *OsHDAC1* expression (Supplemental Figure S4B). *OsHDAC1* OE plants were confirmed by immunoblotting analysis of selected OE lines (Supplemental Figure S4C). For further studies, we selected the lines OE5 and OE6, which displayed the highest *OsHDAC1* expression levels (Supplemental Figure S4B). The

OsHDAC1 RNAi transgenic rice plants were generated by using a pCambia1300 vector that contained two inverted copies of a 202-base pair-specific cDNA fragment of *OsHDAC1* under the control of the 35S promoter (Supplemental Figure S4D). We obtained seven knockdown lines with decreased *OsHDAC1* expression (Supplemental Figure S4E). For further studies, we selected the lines Ri2 and Ri3, which displayed the lowest *OsHDAC1* expression levels. To determine whether the expression levels of homologs of *OsHDAC1* were affected in *OsHDAC1*-RNAi plants, the expression levels of *OsHDAC2* and *OsHDAC3* were determined in *OsHDAC1* Ri2 and Ri3 plants by RT-qPCR (Supplemental Figure S2, A–C). Compared with wild-type plants, the expression level of *OsHDAC1* was markedly reduced in *OsHDAC1*-RNAi plants (Supplemental Figure S4E). No obvious changes were observed in *OsHDAC2* and *OsHDAC3* (Supplemental Figure S4F). Therefore, the *OsHDAC1*-RNAi plants were genuine *OsHDAC1* knockdown transgenic plants.

We examined the LR phenotypes of *OsHDAC1* Ri and OE lines. *OsHDAC1* Ri2 and Ri3 seedlings exhibited fewer LRs on primary roots, compared with wild-type plants. *OsHDAC1* OE5 and OE6 lines showed more LRs on the primary roots (Figure 1A). The LR densities of *OsHDAC1* Ri2 and Ri3 seedlings were decreased compared with the LR density of wild-type plants, while the LR densities of *OsHDAC1* OE5 and OE6 lines were significantly increased (Figure 1B). Taken together, these results indicate that *OsHDAC1* positively regulates LR formation in rice. LR formation requires initiation, patterning, and emergence. We thus examined the emergence of LR primordia (LRPs) on the seedling primary roots via methylene blue staining. Many intensely stained regions, indicating the presence of LRP, were visible on the primary root of 5-day-old seedlings overexpressing *OsHDAC1*, whereas staining was less intense in *OsHDAC1* Ri2 and Ri3 plants than in wild-type rice seedling roots (Figure 1, C and D). These results suggest that *OsHDAC1* regulates LR number by modulating LRP initiation.

OsHDAC1 physically interacts with OsGSK2

To investigate the mechanism underlying *OsHDAC1*-mediated LR formation, we attempted to identify its deacetylation target(s) and other interacting proteins in a yeast screening assay. *OsHDAC1* could interact with *OsGSK2*, a GSK3/SHAGGY-like kinase, as shown by yeast two-hybrid assay (Figure 2A). *OsGSK2* negatively regulates BR signaling by inhibiting the activity of *OsBZR1* (Tong et al., 2012). BRs promote LR development by increasing acropetal auxin transport in *Arabidopsis* (Bao et al., 2004). Thus, we speculated that *OsGSK2* was a potential interactor for *OsHDAC1*-mediated LR formation.

To confirm this hypothesis, we evaluated the physical interaction between *OsHDAC1*-nLUC and cLUC-*OsGSK2* using a luciferase complementation imaging assay. After the *OsHDAC1*-nLUC and cLUC-*OsGSK2* vector pairs were co-expressed in *Nicotiana benthamiana* leaves, we detected luciferase activity in the *OsHDAC1* and *OsGSK2* combination,

but not in the negative control combinations (Figure 2B). These findings suggest that *OsHDAC1* interacts with *OsGSK2* in *N. benthamiana*. Furthermore, *OsHDAC1*-HA and *OsGSK2*-MYC were co-expressed in rice protoplasts and subjected to coimmunoprecipitation analysis. *OsGSK2*-MYC co-purified with *OsHDAC1*-HA using an anti-HA antibody, but no *OsGSK2*-MYC was obtained from the control (Figure 2C). We conclude that *OsHDAC1* interacts with *OsGSK2* in vivo. In addition, for in vitro interaction assays, we purified recombinant GST-*OsHDAC1* and *OsGSK2*-His proteins from *Escherichia coli* (BL21) to conduct GST-pull-down assays (Supplemental Figure S5). *OsGSK2*-His was pulled down by GST-*OsHDAC1* but not by GST (Figure 2D). Taken together, these in vivo and in vitro results suggest that *OsHDAC1* physically interacts with *OsGSK2*.

OsGSK2 negatively regulates LR formation in rice

To determine whether *OsGSK2* is involved in rice LR development, we generated loss-of-function and gain-of-function transgenic plants. We used clustered regularly interspaced short palindromic repeats (CRISPR)/CRISPR-associated (Cas) protein 9 system to create *OsGSK2* knockout mutants, by selecting one site in the fourth exon for small guide RNA (sgRNA) design (Figure 3A). Among the mutant lines isolated, *osgsk2-1* had a single-nucleotide deletion and *osgsk2-2* had a five-nucleotide deletion at the sgRNA site (Figure 3A). Each mutation causes a frameshift in the *OsGSK2* coding sequence that disrupts translation by generating a premature stop codon. In addition, transgenic rice plants overexpressing *OsGSK2* were generated using a pCXUN vector that contained *OsGSK2* cDNA fused to the MYC tag under the control of the ubiquitin promoter (Supplemental Figure S6A). We obtained 10 lines with increased *OsGSK2* expression (Supplemental Figure S6B); overexpression of *OsGSK2* was confirmed by immunoblotting analysis of selected OE lines (Supplemental Figure S6C). For further studies, we selected the lines OE5 and OE10, which had the highest *OsGSK2* expression levels.

The phenotypes of *OsGSK2* mutant and OE lines were evaluated. We found that *osgsk2-1* and *osgsk2-2* seedlings exhibited more LRs on primary roots than did wild-type plants, whereas *OsGSK2* OE5 and OE10 plants showed fewer LRs on the primary roots (Figure 3B). The LR densities of *osgsk2-1* and *osgsk2-2* seedlings were significantly increased, compared with the LR density of the wild-type plants, while the LR densities of *OsGSK2* OE5 and OE10 plants were significantly decreased (Figure 3D). Taken together, these results indicate that *OsGSK2* negatively regulates LR formation in rice. Methylene blue staining showed that more LRPs were visible on the primary root in the *osgsk2-1* and *osgsk2-2* seedlings and less in *OsGSK2* OE5 and OE10 plants, compared with wild-type rice seedlings (Figure 3, C and E). These results suggest that *OsGSK2* and *OsHDAC1* have opposite functions during LR formation in rice.

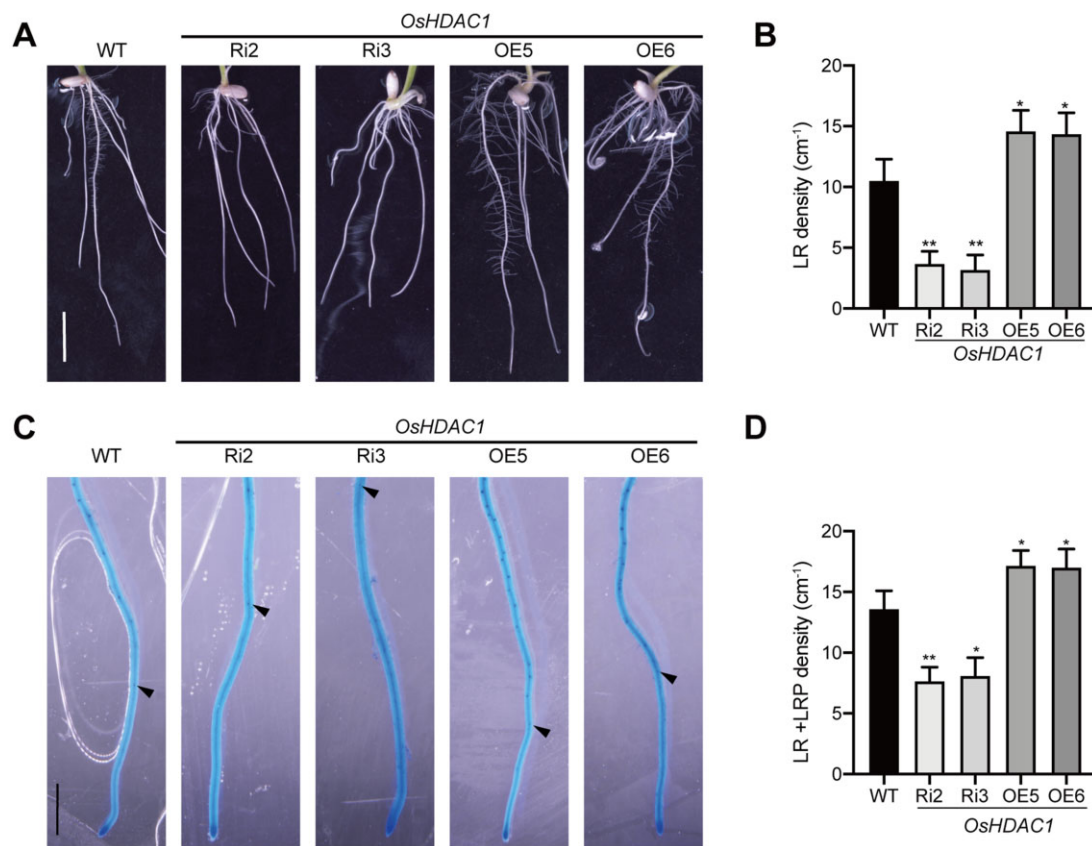


Figure 1 OsHDAC1 promotes LR formation. A, Phenotype of roots in 5-day-old seedlings of WT, *OsHDAC1* Ri2, Ri3, OE5, and OE6 plants. Scale bar = 1 cm. B, LR densities of WT, *OsHDAC1* Ri2, Ri3, OE5, and OE6 plants. Values are means \pm SD ($n = 20$ plants). Asterisks mark significant changes compared with WT based on Student's *t* test: * $P < 0.05$, ** $P < 0.01$. C, Methylene blue staining showed LRPs in a segment of the root-tip of 5-day-old seedlings of WT, *OsHDAC1* Ri2, Ri3, OE5, and OE6 plants. Scale bar = 2 mm. D, LR + LRP densities of WT, *OsHDAC1* Ri2, Ri3, OE5, and OE6 plants. Values are mean \pm SD ($n = 20$ plants). Asterisks mark significant changes compared with WT based on Student's *t* test: * $P < 0.05$, ** $P < 0.01$. WT, wild-type rice; OE, *OsHDAC1*-overexpressing lines; Ri, *OsHDAC1*-RNAi lines.

OsHDAC1 deacetylates OsGSK2 and inhibits its kinase activity

BIN2, an ortholog of OsGSK2, is deacetylated in Arabidopsis (Hao et al., 2016). To examine whether OsGSK2 can be deacetylated by OsHDAC1, the deacetylation activity of purified GST-OsHDAC1 fusion protein was evaluated using a deacetylation assay. In the presence of the same amount of the substrate Kac-peptide, the absorbance was increased by the addition of GST-OsHDAC1 (Figure 4A), demonstrating that OsHDAC1 possesses deacetylation activity *in vitro*.

To confirm *in vitro* deacetylation of OsGSK2 proteins by OsHDAC1, *in vitro*-purified OsGSK2-His fusion protein was incubated with or without GST-OsHDAC1 in deacetylation buffer. In the absence of GST-OsHDAC1, OsGSK2-His showed a high level of lysine acetylation, indicating that the proteins were acetylated in *E. coli* cells (Figure 4B). The presence of OsHDAC1 reduced their lysine acetylation levels (Figure 4B). Furthermore, we incubated the immunoprecipitated OsGSK2-MYC protein produced in OsGSK2 OE lines with or without *E. coli*-produced GST-OsHDAC1. Incubation with GST-OsHDAC1 reduced the lysine acetylation level of OsGSK2-MYC, indicating that OsGSK2 was acetylated in rice and could be deacetylated by OsHDAC1 *in vitro* (Figure 4C).

As the prior study has shown that BIN2 activity is regulated by deacetylation in Arabidopsis (Hao et al., 2016), we hypothesized that OsHDAC1 modulates OsGSK2 activity via deacetylation. As expected, OsGSK2-His activity in the presence of GST-OsHDAC1 was significantly decreased compared with the absence of GST-OsHDAC1 (Figure 4D), suggesting that OsGSK2 activity is inhibited by OsHDAC1 via deacetylation. To confirm these results, we tested the *in vivo* deacetylation of OsGSK2 by OsHDAC1. We immunoprecipitated OsGSK2 protein from wild-type, *OsHDAC1* Ri2, Ri3, OE5, and OE6 plants using an anti-GSK2 antibody. We then analyzed OsGSK2 lysine acetylation levels by immunoblotting using an anti-LysAc antibody. Higher and lower levels of OsGSK2 lysine acetylation were detected in *OsHDAC1* Ri and OE lines, respectively, compared with wild-type plants (Figure 4E). Therefore, OsGSK2 could be acetylated and deacetylated by OsHDAC1 in rice plants. In addition, the immunoprecipitated OsGSK2 proteins were used to examine the activity of OsGSK2. OsGSK2 activity was increased in *OsHDAC1* Ri plants and decreased in OE plants, compared with wild-type plants (Figure 4F). These results suggest that OsHDAC1 deacetylates OsGSK2 to inhibit its kinase activity in rice plants.

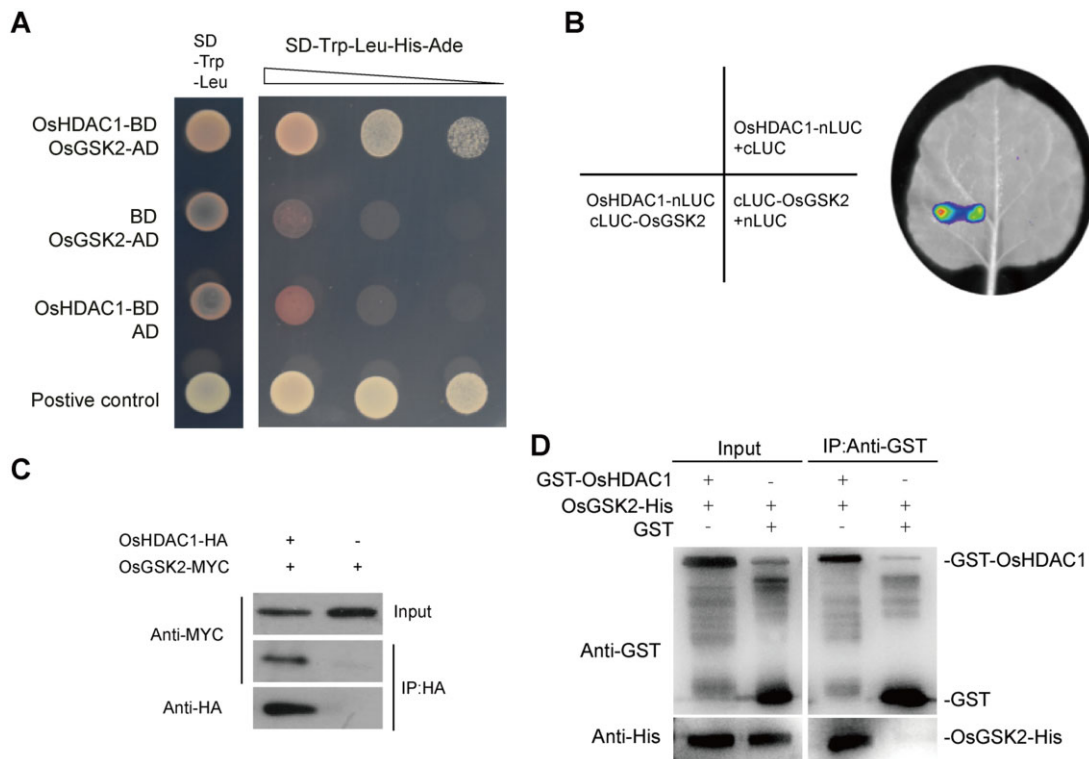


Figure 2 OsHDAC1 interacts with OsGSK2. **A**, Yeast two-hybrid assays showed that OsHDAC1 interacts with OsGSK2 in yeast. Empty pGBKT7/OsGSK2-AD and empty pGADT7/OsHDAC1-BD were the negative controls, respectively; co-transfer of pGBKT7-53 and pGADT7-T (Clontech) was used the positive control. **B**, Luciferase complementation imaging assays showed that OsHDAC1 interacted with OsGSK2 in *N. benthamiana* leaves. Empty nLUC and cLUC were used as negative controls. **C**, Coimmunoprecipitation assays showed that OsHDAC1 interacted with OsGSK2 in rice protoplast. **D**, Pull-down assays showed that OsHDAC1 interacted with OsGSK2 *in vitro*. The GST tag was used as the negative control. + or -, presence or absence of protein. SD, synthetic dropout medium; BD, binding domain; AD, activation domain; LUC, luciferase gene; IP, immunoprecipitation; HA, HA epitope tag sequence; MYC, MYC epitope tag sequence; GST, GST epitope tag sequence; His, His epitope tag sequence.

OsHDAC1 contributes to BR-induced rice LR formation

Low concentrations of brassinolide (BL) reportedly promote LR formation in Arabidopsis (Bao et al., 2004). We applied 1, 10, 100, and 1,000-nM BL to wild-type plants for 5 d and evaluated the role of BL in the regulation of rice seedling LR formation. BL increased LR formation (Supplemental Figure S7, A and B). We also used methylene blue staining to examine the emergence of LRPs from seedling primary roots that had been treated with exogenous BL for 5 d. The numbers of signal dots, indicating LRPs, were significantly increased on the BL-treated primary root, compared with the untreated primary root (Supplemental Figure S7, C and D). Because higher concentrations of BL inhibited primary root growth, 10 nM was used in subsequent experiments. Therefore, BR regulates LR formation in rice.

The findings that BL promotes LRP formation to increase the number of LRs, and that OsHDAC1 and OsGSK2 are involved in LR formation in rice, prompted us to assess the contribution of OsHDAC1 to BR-induced LR formation. Treatment of *OsHDAC1* Ri2 and Ri3 seedlings with BL yielded little or no increase in the LR number, compared with untreated RNAi rice seedlings (Figure 5, A and B). BRs directly regulate BIN2 through the BRI1 plasma membrane receptor

in Arabidopsis (Kim et al., 2009). Therefore, we hypothesized that OsHDAC1 is involved in BRs by regulating OsGSK2 in rice. To test this hypothesis, we examined the mRNA levels of *OsHDAC1* in wild-type plants that had or had not been treated with BL. *OsHDAC1* was significantly upregulated in response to BL (Figure 5C). Furthermore, we examined the activity of OsGSK2 in *OsHDAC1* Ri and wild-type plants in response to BL treatment. As expected, OsGSK2 activity was unchanged in *OsHDAC1* Ri2 and Ri3 plants that had been treated with BL, whereas OsGSK2 activity in wild-type plants was significantly decreased in response to BL (Figure 5D). We next used Bikinin, an inhibitor of GSK3/SHAGGY-like kinases, to treat *OsHDAC1*-knockdown plants. Compared with wild-type rice, these RNAi lines showed increased LR formation (Figure 5, A and B). In *OsHDAC1* RNAi seedlings, Bikinin but not BL induced LR formation. This finding indicates that OsHDAC1 regulates BR-induced LR formation by deacetylating OsGSK2 and other GSK3/SHAGGY-like kinases.

OsHDAC1 promotes OsBZR1 accumulation in an OsGSK2-dependent manner

Considering that OsBZR1 is a downstream transcription factor of the BR pathway, which is phosphorylated by OsGSK2

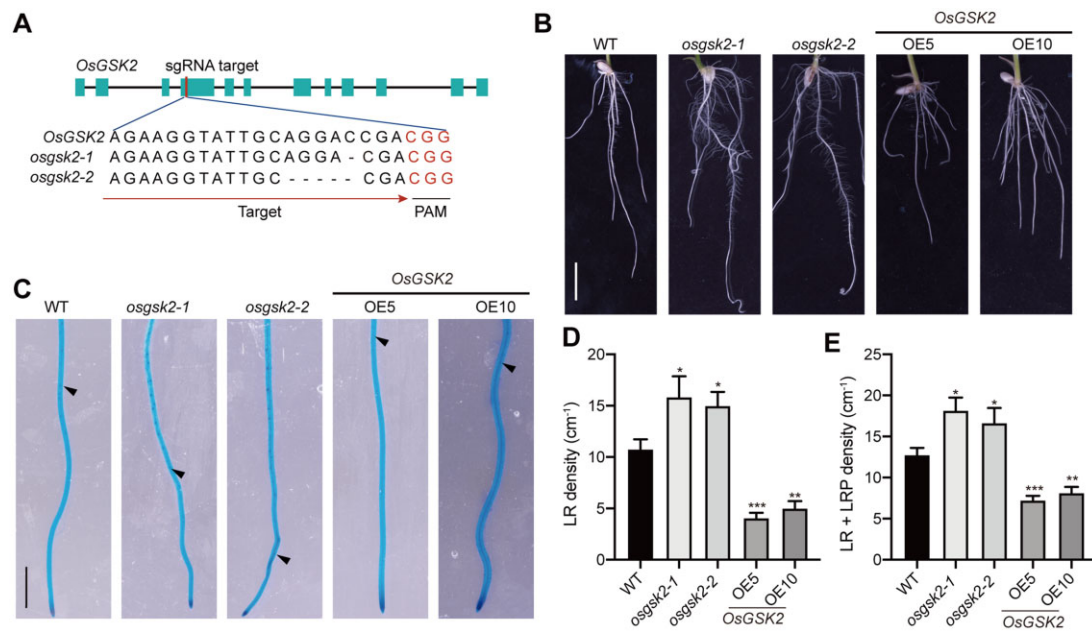


Figure 3 OsGSK2 inhibits LR formation. A, Gene structure and mutation sites of *OsGSK2*. sgRNA, small guide RNA; PAM, protospacer adjacent motif. B, Phenotype of roots in 5-d-old seedlings of WT, *osgsk2-1*, *osgsk2-2*, *OsGSK2* OE5, and OE10 plants. Scale bars = 1 cm. C, Methylene blue staining of LRPs in a segment of the root-tip of 5-d-old seedlings of WT, *osgsk2-1*, *osgsk2-2*, *OsGSK2* OE5, and OE10 plants. Scale bar = 2 mm. D, LR densities and (E) LR + LRP densities of WT, *osgsk2-1*, *osgsk2-2*, *OsGSK2* OE5, and OE10 plants. Values are mean \pm SD ($n = 20$ plants). Asterisks mark significant changes compared with WT based on Student's *t* test: * $P < 0.05$, ** $P < 0.01$, *** $P < 0.001$. WT, wild-type rice; OE, *OsGSK2*-over-expressing lines.

and destabilized (Tong et al., 2012), we next examined whether *OsHDAC1* affects the interplay between *OsGSK2* and *OsBZR1*. Yeast three-hybrid assay analysis showed that the *OsBZR1*–*OsGSK2* interaction was suppressed in yeast cells expressing *OsHDAC1* (Figure 6A). Trichostatin A (TSA) is an HDAC inhibitor, which can inhibit the activity of HDACs in vivo and in vitro (Tanaka et al., 2008). In coimmunoprecipitation assays, *OsBZR1*-Flag was co-expressed with *OsGSK2*-MYC in rice protoplasts with or without TSA treatment; *OsBZR1*-Flag was detected in a complex immunoprecipitated using an anti-FLAG antibody (Figure 6B). When *OsHDAC1*-HA was co-expressed with *OsBZR1*-Flag and *OsGSK2*-MYC in rice protoplasts, the amount of immunoprecipitated *OsBZR1*-Flag was lower than in the absence of *OsHDAC1*, whereas the amount of immunoprecipitated *OsBZR1*-Flag was increased by TSA treatment (Figure 6B). Therefore, *OsHDAC1* disrupted the *OsBZR1*–*OsGSK2* interaction in vivo.

This conclusion was supported by the results of in vitro pull-down assays. Purified GSK2-His and MBP-*OsBZR1* were incubated with or without GST-*OsHDAC1* in deacetylation buffer for 3 h to conduct His-pull-down assays. Coprecipitation of MBP-*OsBZR1* with *OsGSK2*-His was largely prevented by incubation with GST-*OsHDAC1* (Figure 6C). Addition of the HDAC-inhibitor TSA partially restored the binding of MBP-*OsBZR1* to *OsGSK2*-His in the presence of GST-*OsHDAC1* (Figure 6C). These data, combined with the results of the coimmunoprecipitation assays, demonstrated that the *OsHDAC1*-mediated deacetylation of *OsGSK2*

attenuates the association between *OsGSK2* and *OsBZR1*. Next, to determine whether deacetylated *OsGSK2* prevents *OsBZR1* degradation in plants, we compared the abundance of *OsBZR1* protein in wild-type, *OsHDAC1* Ri2, Ri3, OE5, and OE6 plants. The level of *OsBZR1* was increased in *OsHDAC1* OE lines (Figure 6D). In contrast, *OsBZR1* proteins were reduced in *OsHDAC1* RNAi lines, compared with wild-type plants (Figure 6E). These results indicate that *OsHDAC1* stabilizes *OsBZR1* by deacetylating *OsGSK2*.

OsHDAC1-mediated OsBZR1 stabilization to regulate LR formation

BZR1/BES1 in *Arabidopsis* is important for the control of LR development (Xu et al., 2020). To investigate the function of *OsBZR1* in rice LR development, we generated *OsBZR1* gain-of-function transgenic plants by using a pCXUN vector that contained *OsBZR1* cDNA fused to the FLAG tag under the control of the ubiquitin promoter (Supplemental Figure S8A). We obtained nine OE lines with increased *OsBZR1* expression (Supplemental Figure S8B). *OsBZR1* OE was confirmed by immunoblotting analysis of selected OE lines (Supplemental Figure S8C). For further studies, we selected the lines OE4 and OE8, which displayed the highest *OsBZR1* expression levels (Supplemental Figure S8B). The *OsBZR1* OE4 and OE8 lines had more LRs on the primary roots than did wild-type plants (Figure 7, A and B). Methylene blue staining showed greater numbers of stained dots in *OsBZR1* OE4 and OE8 plants, compared with wild-type rice seedling roots (Figure 7, C and D). Taken together, these results

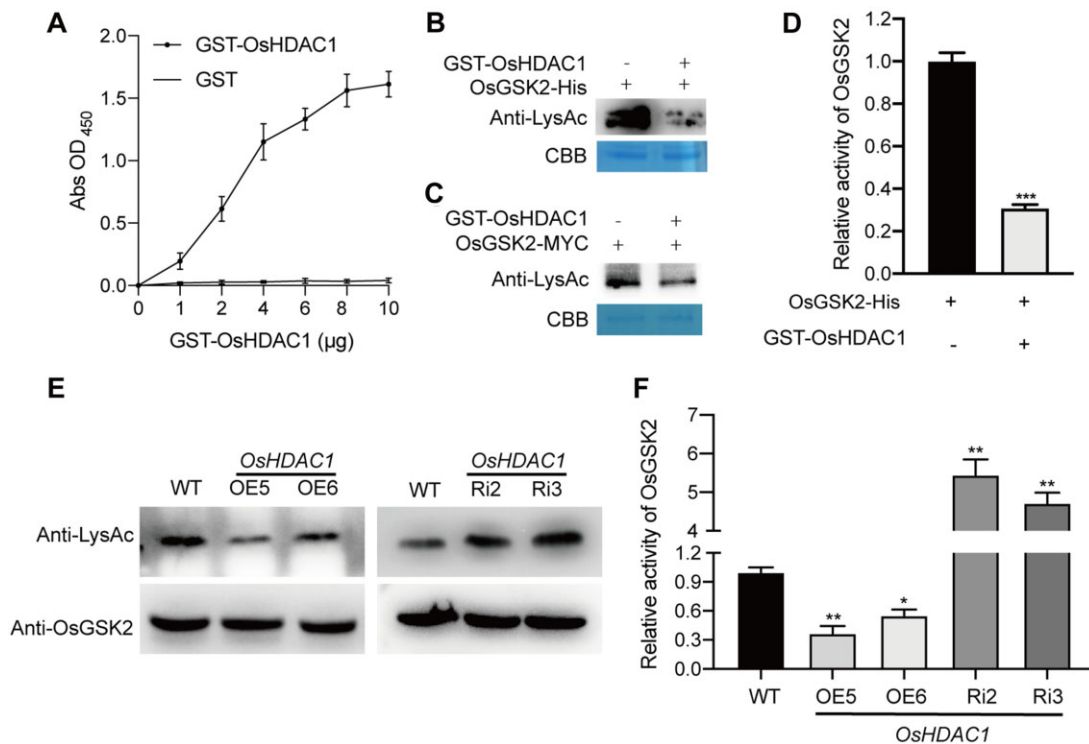


Figure 4 OsHDAC1 deacetylates OsGSK2 and inhibits its kinase activity. A, OsHDAC1 has deacetylation activity in vitro. The GST-OsHDAC1 fusion protein was expressed and purified in *E. coli* for deacetylase activity assays; the catalytic rate of OsHDAC1 was represented by the absorbance of the reaction at 450 nm. B, In vitro deacetylation assays of OsGSK2 from *E. coli*. The purified OsGSK2-His protein was incubated with (+) or without (-) GST-OsHDAC1 in deacetylation buffer and analyzed by immunoblotting using an anti-LysAc antibody. CBB staining was used as a protein loading control. C, In vitro deacetylation assays of OsGSK2-MYC from plants. OsGSK2-MYC proteins immunoprecipitated from OsGSK2 OE5 seedlings were incubated with (+) or without (-) GST-OsHDAC1 in deacetylation buffer and analyzed using an anti-LysAc antibody. CBB staining was used as a protein loading control. D, OsHDAC1 inhibits OsGSK2 activity in vitro. Recombinant OsGSK2-His protein was purified from *E. coli*; OsGSK2-His activity was measured with (+) or without (-) GST-OsHDAC1 in deacetylation buffer. Values are mean \pm SD ($n = 3$). Asterisks mark significant changes compared with WT based on Student's *t* test: *** $P < 0.001$. E, Effects of *OsHDAC1* loss- or gain-of-function on lysine acetylation of OsGSK2 in vivo in rice plants. OsGSK2 was immunoprecipitated from *OsHDAC1* Ri2, Ri3, OE5, OE6, and WT plants by anti-OsGSK2 and analyzed by immunoblotting using the indicated antibodies. Anti-OsGSK2 was used as a protein loading control. F, OsGSK2 activity of roots in 5-d-old seedlings of WT, *OsHDAC1* Ri2, Ri3, OE5, and OE6 plants. The activity of OsGSK2 in the WT was set to 1. Values are mean \pm SD ($n = 3$). Asterisks mark significant changes compared with WT based on Student's *t* test: * $P < 0.05$, ** $P < 0.01$. GST, GST epitope tag sequence; His, His epitope tag sequence; MYC, MYC epitope tag sequence; WT, wild-type rice; OE, *OsHDAC1*-overexpressing lines; Ri, *OsHDAC1*-RNAi lines.

suggest that OsBZR1 regulates LRP formation to increase the number of LRs.

Arabidopsis BZR1 controls the expression of several signaling components of the auxin/IAA signaling pathway (Sun et al., 2010). In rice, *OsIAA11* negatively regulates LR growth (Jing et al., 2015) and *OsIAA13* enhances LR growth (Kitomi et al., 2012). Therefore, we investigated the expression of *OsIAA11* and *OsIAA13* in *OsBZR1* OE lines. *OsIAA11* was significantly downregulated and *OsIAA13* was significantly upregulated in *OsBZR1* OE4 and OE8 plants, compared with wild-type plants (Figure 7E). As expected, *OsIAA11* expression was significantly increased and *OsIAA13* expression was significantly decreased in *OsGSK2* OE5 and OE10 plants, compared with wild-type plants; *OsIAA11* expression was significantly decreased and *OsIAA13* expression was significantly increased in *osgsk2-1* and *osgsk2-2* plants (Figure 7F).

These results imply that the *OsGSK2*/*OsBZR1* module controls LR formation by modulating the expression of LR formation-related genes (e.g. *OsIAA11* and *OsIAA13*). Next, the expression levels of *OsIAA11* and *OsIAA13* were measured in *OsHDAC1* transgenic rice plants. The mRNA level of *OsIAA11* was higher in *OsHDAC1* RNAi plants and lower in *OsHDAC1* OE plants, compared with wild-type plants; *OsIAA13* expression showed the opposite pattern in *OsHDAC1* transgenic rice plants (Figure 7G). The exogenous application of Bixin significantly decreased *OsIAA11* expression and increased *OsIAA13* expression, even in *OsHDAC1* RNAi plants (Figure 7H); these effects were similar to results of *OsGSK2* mutation. Therefore, *OsHDAC1* positively regulates *OsBZR1* by inactivating *OsGSK2*, thus inducing the expression of LR formation-related genes and LR development.

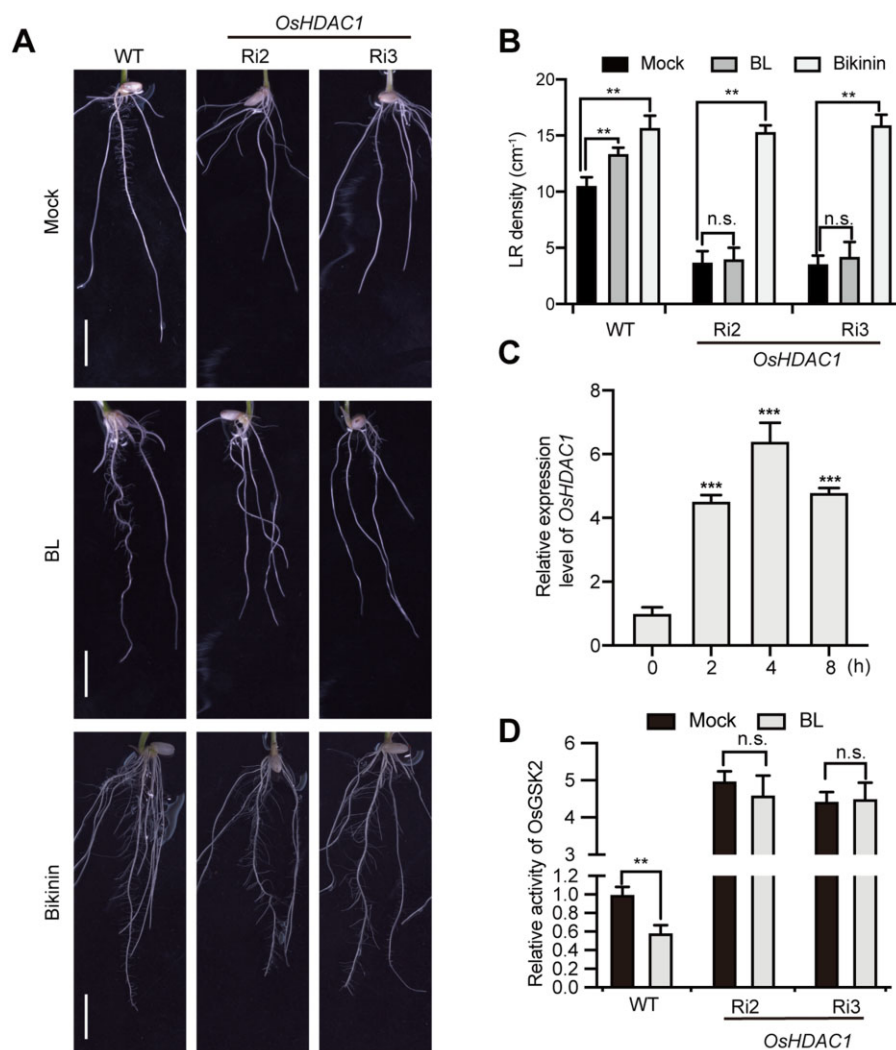


Figure 5 *OsHDAC1* contributes to BR-induced rice LR formation by *OsGSK2*. A, Phenotype of LR formation of 5-d-old WT, *OsHDAC1* Ri2, and Ri3 seedlings grown on Murashige and Skoog medium with 10-nM BL and 5- μ M Bikinin. Scale bar = 1 cm. B, LR densities of WT, Ri2, and Ri3 plants with or without 10-nM BL and 5- μ M Bikinin. Values are mean \pm SD ($n = 20$ plants). Asterisks mark significant changes compared with WT, Ri2, or Ri3 without 10-nM BL and 5- μ M Bikinin treatment based on Student's t test: ** $P < 0.01$. n.s., no significant change. C, Expression of *OsHDAC1* in the WT treated with 10-nM BL for 0, 2, 4, and 8 h. Total RNA was extracted from the root tips of WT and subjected to RT-qPCR. The expression levels of genes in the WT without BL treatment were set to 1. Values are mean \pm SD ($n = 3$). Asterisks mark significant changes compared with WT plants without BL treatment based on Student's t test: *** $P < 0.001$. D, *OsGSK2* activity of roots in 5-d-old seedlings of WT, *OsHDAC1* Ri2, and Ri3 plants with or without 10-nM BL treatment. *OsGSK2* activity in the WT without 10-nM BL treatment was set as 1. Values are mean \pm SD ($n = 3$). Asterisks mark significant changes compared with WT plants with 10-nM BL treatment based on Student's t test: ** $P < 0.01$. n.s., no significant change; WT, wild-type rice; Ri, *OsHDAC1*-RNAi lines.

Discussion

LR formation is a key determinant of the root system architecture; thus, understanding the molecular mechanism that regulates LR formation in rice (*O. sativa* L.) is of great agronomic value. We identified *OsHDAC1* as a positive regulator and *OsGSK2* as a negative regulator of LR formation in rice. *OsHDAC1* regulated LR formation in rice by interacting with and deactivating *OsGSK2*, which prevented *OsBZR1* degradation and led to the expression of downstream LR formation genes. Thus, our data support a model in which *OsHDAC1* regulates BR-mediated LR formation through *OsGSK2*/*OsBZR1* in rice (Figure 8).

HDACs transcriptionally regulate gene expression by removing acetyl groups from histones, resulting in various physiological changes. In *Arabidopsis*, HD2A and HD2B are recruited to the promoters of target genes and repress their transcription (Wu et al., 2010). HDACs catalyze the removal of acetyl groups from both histones and acetylated nonhistone proteins; these activities have vital roles in animal cell metabolic and plant development regulation (Hao et al., 2016; Narita et al., 2019). Rice *OsHDAC1* is an RPD3-type deacetylase, similar to HDA19 in *Arabidopsis*. *OsHDAC1* controls seedling root growth in rice (Chung et al., 2009). To investigate the role of *OsHDAC1* in protein deacetylation and root development, we generated *OsHDAC1* loss-of-function

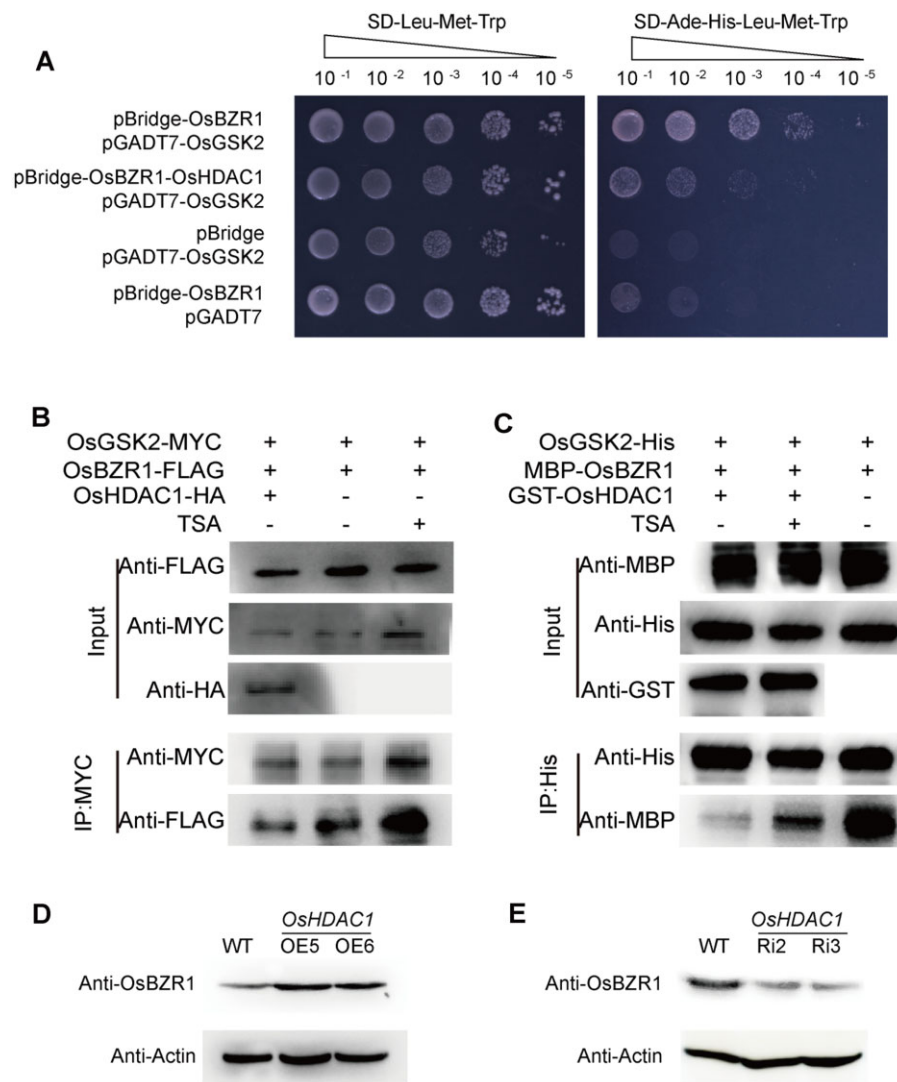


Figure 6 OsHDAC1 inhibits the interaction between OsGSK2 and OsBZR1. A, Yeast three-hybrid assays of the effect of OsHDAC1 on the OsGSK2-OsBZR1 interaction. Empty pBridge and pGADT7 were used as negative controls. B, In vivo coimmunoprecipitation assays showed that OsHDAC1 prevented the interaction of OsGSK2 and OsBZR1. Total proteins extracted from rice protoplasts co-expressing OsHDAC1-HA, OsGSK2-MYC, OsBZR1-FLAG or OsGSK2-MYC, and OsBZR1-FLAG with (+) or without (-) 0.1- μ M TSA treatment were immunoprecipitated by an anti-MYC antibody. OsBZR1-FLAG was used as a loading control. C, In vitro pull-down assays showed that GST-OsHDAC1 inhibited the interaction between OsGSK2-His and MBP-OsBZR1. Purified OsGSK2-His and MBP-OsBZR1 proteins were incubated with purified GST-OsHDAC1 protein in reaction buffer with (+) or without (-) 0.1- μ M TSA. MBP-OsBZR1 was used as a loading control. D, OsBZR1 protein levels in WT, *OsHDAC1* OE5, and OE6 plants. Actin was used as a loading control. E, OsBZR1 protein levels in WT, *OsHDAC1* Ri2, and Ri3 plants. Actin was used as a loading control. IP, immunoprecipitation; MYC, MYC epitope tag sequence; HA, HA epitope tag sequence; FLAG, FLAG epitope tag sequence; MBP, MBP epitope tag sequence; His, His epitope tag sequence; GST, GST epitope tag sequence; TSA, trichostatin A; WT, wild-type rice; OE, *OsHDAC1*-overexpressing lines; Ri, *OsHDAC1*-RNAi lines.

mutants using the CRISPR/Cas9 system. However, although we propagated several generations, we did not generate homozygous seeds. This is consistent with the approach in a previous study, which used heterozygous *OsHDAC1* KO plants because the authors could not obtain homozygous seeds, despite selection for several generations (Jang et al., 2003). Therefore, we generated *OsHDAC1* RNAi transgenic rice lines (Supplemental Figure S4, D–F). These knockdown lines demonstrated decreased *OsHDAC1* expression; they also exhibited fewer LR than did wild-type rice plants. We constructed transgenic rice plants overexpressing *OsHDAC1*,

which showed increased *OsHDAC1* expression and increased LR formation (Supplemental Figure S4, A–C; Figure 1, A–D). Therefore, *OsHDAC1* is a positive regulator of LR formation in rice.

Auxin is a key regulator of plant LR formation. Genetic analysis of a *bri1* mutant defective in the BR receptor, which showed fewer LR compared with wild-type rice, indicated that BR interacts with auxin to promote LR development in Arabidopsis (Bao et al., 2004). Little is known regarding how the BR signaling pathway participates in plant LR formation. Multiple components of the BR signaling pathway have

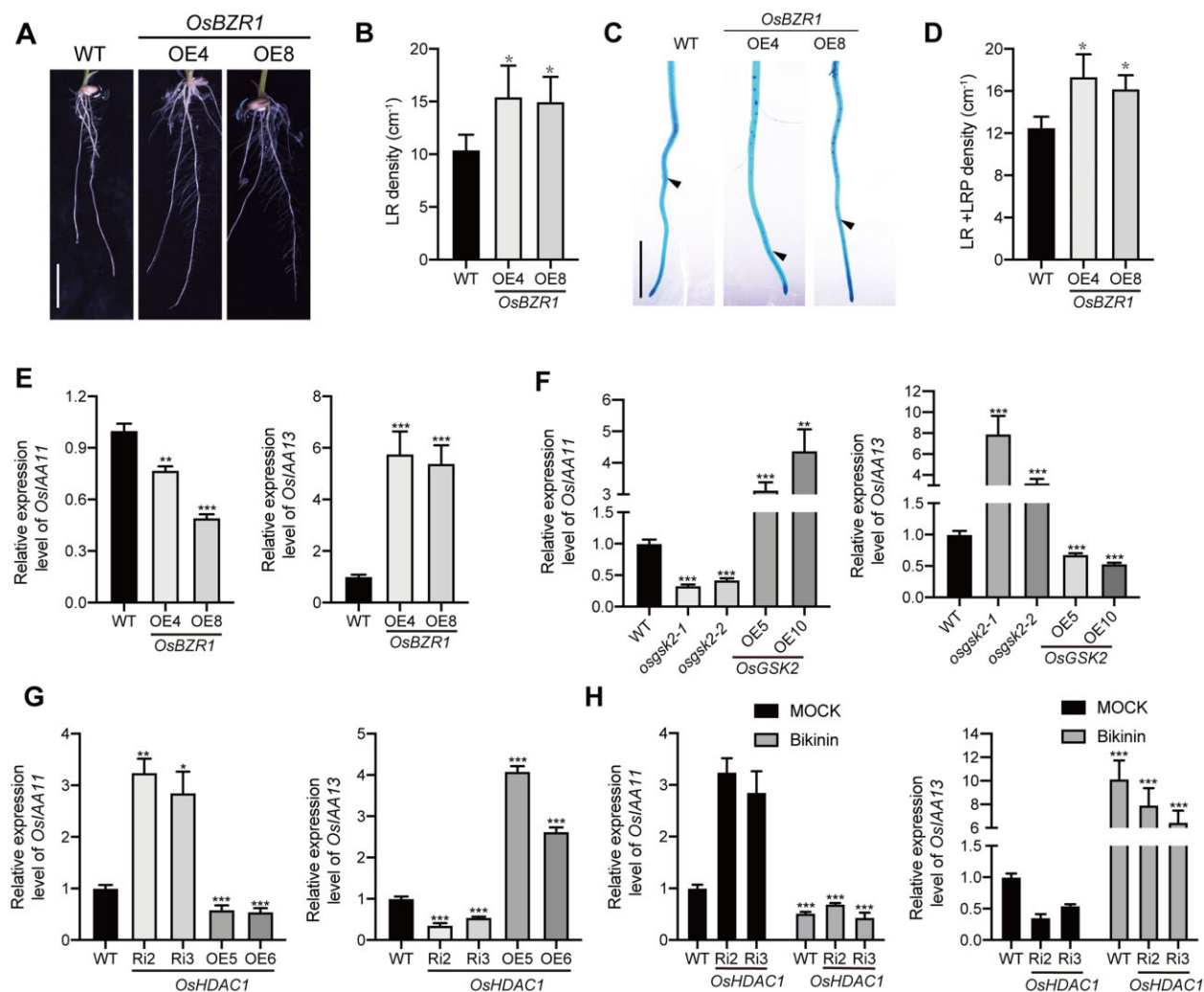


Figure 7 The OsHDAC1/OsGSK2/OsBZR1 module mediates the expression of LR formation-related genes and LR formation. A, Phenotype of roots in 5-d-old seedlings of WT, *OsBZR1* OE4, and OE8 plants. Scale bar = 1 cm. B, LR densities of WT, *OsBZR1* OE4, and OE8 plants. Values are mean \pm SD ($n = 20$ plants). Asterisks mark significant changes compared with WT based on Student's *t* test: * $P < 0.05$. C, Methylene blue staining of LRPs in a segment from the root-tip of 5-d-old seedlings of WT, *OsBZR1* OE4, and OE8 plants. Scale bar = 1 mm. (D) LR + LRP densities of WT, *OsBZR1* OE4, and OE8 plants. Values are mean \pm SD ($n = 20$ plants). Asterisks mark significant changes compared with WT based on Student's *t* test: * $P < 0.05$. E, Expression of *OsIAA11* and *OsIAA13* in WT, *OsBZR1* OE4, and OE8 plants. F, Expression of *OsIAA11* and *OsIAA13* in WT, *osgsk2-1*, *osgsk2-2*, *OsGSK2* OE5, and OE10 plants. G, Expression of *OsIAA11* and *OsIAA13* in WT, *OsHDAC1* Ri2, Ri3, OE5, and OE6 plants. H, Expression of *OsIAA11* and *OsIAA13* in WT, *OsHDAC1* Ri2, and Ri3 plants with or without Bikinin treatment. Total RNA was extracted from root tips and subjected to RT-qPCR. The expression levels of genes in the WT were set to 1.00. Values are mean \pm SD ($n = 3$). Asterisks mark significant changes compared with WT or WT without Bikinin treatment based on Student's *t* test: * $P < 0.05$, ** $P < 0.01$, *** $P < 0.001$. WT, wild-type rice; OE, *OsBZR1* or *OsGSK2*-overexpressing lines; Ri, *OsHDAC1*-RNAi lines.

been identified in rice (Tong et al., 2012; Qiao et al., 2017). Bioinformatics analysis revealed that there are nine genes that encode GSK3/SHAGGY-like kinases in the rice genome (Youn and Kim, 2015). *OsGSK2* functions as a key negative regulator in the BR signaling pathway and has important roles in linking many other signaling pathways. In Arabidopsis, the phosphatase BSU1 may dephosphorylate BIN2 to inhibit its kinase activity (Kim et al., 2009), and HDA6 deacetylates and inhibits BIN2 (Hao et al., 2016). Thus, BIN2 may be regulated by multiple protein modifications, such as phosphorylation and acetylation, in Arabidopsis. Exogenous BL treatment led to a significant

increase in *OsHDAC1* expression, whereas the treatment of *OsHDAC1*-knockdown seedlings with BL did not increase the LR number, compared with untreated *OsHDAC1*-knockdown seedlings (Figure 5, A–C). These results implicate *OsHDAC1* in BR signaling to induce LR formation by inactivating *OsGSK2* in rice.

In vitro and in vivo molecular experiments showed that *OsHDAC1* directly interacts with and deacetylates *OsGSK2* (Figure 2, A–D and Figure 4, B, C, and E). Thus, our results suggest that rice has a conserved HDAC-mediated *OsGSK2* deacetylation mechanism in the BR signaling pathway, similar to Arabidopsis. Arabidopsis HDA6 interacts directly with

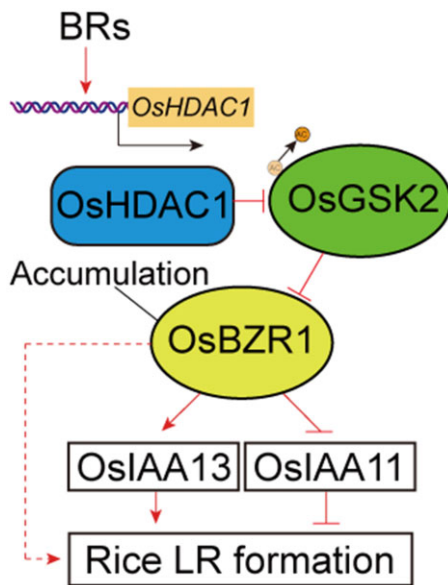


Figure 8 Proposed model of OsHDAC1/OsGSK2/OsBZR1 module-mediated LR formation in rice. Exogenous application of BRs upregulates OsHDAC1, which binds to and deacetylates OsGSK2 to inhibit its kinase activity. Deacetylated OsGSK2 loses its binding and kinase activities for the transcription factor OsBZR1, leading to the accumulation of OsBZR1. Stable OsBZR1 controls LR formation by inducing the expression of *OsIAA13* and inhibiting the expression of *OsIAA11*.

BES1 (Hao et al., 2016) but our results showed that OsHDAC1 did not interact with OsBZR1 (Supplemental Figure S9). Furthermore, our phylogenetic analysis showed 78.60% sequence similarity between OsHDAC1 and Arabidopsis HDA19 (Supplemental Figure 2, A–C). Therefore, different plants might use specific HDACs to regulate GSK3/SHAGGY-like kinases.

Notably, OsGSK2 mutants had opposite phenotypes to OsHDAC1 mutants with respect to LR numbers, showing increased LR formation (Figure 3, A–E). The analysis of OsGSK2 kinase activity showed that the OsHDAC1–OsGSK2 interaction promoted the deacetylation of OsGSK2 and repressed its kinase activity in vitro (Figure 2, D and Figure 4, B–D). Assays in OsHDAC1 overexpressing plants revealed that an interaction between OsHDAC1 and OsGSK2 in rice plants promoted the deacetylation of OsGSK2 and suppressed its kinase activity (Figure 2, C and Figure 4, E and F). These data suggest that OsHDAC1 acts with OsGSK2 to control LR formation. This conclusion was supported by the observation that inhibition of GSK3/SHAGGY-like kinase activity caused LR formation in *OsHDAC1* RNAi plants and in wild-type rice, even in the absence of exogenous BL (Figure 5, A and B). The findings concerning the effects of OsHDAC1, OsGSK2, and OsBZR1 on LR formation-related genes support our conclusion (Figure 7, E–H).

OsGSK2 interacts with OsBZR1, a transcription factor, and is responsible for its degradation (Tong et al., 2012). The deacetylation of OsGSK2 by OsHDAC1 is important for regulating OsGSK2 kinase activity and its binding to OsBZR1 in

rice. In the absence of OsHDAC1, OsGSK2 has kinase activity and interacted with OsBZR1. In the presence of OsHDAC1 (Figure 6, A–C), OsHDAC1 binds to and deacetylates OsGSK2 to inhibit its kinase activity, leading to the accumulation of OsBZR1 (Figure 6E). Overexpression of OsBZR1 increased LR formation (Figure 7, A–D). Chip-seq and RNA-seq data in Arabidopsis revealed that BZR1 could regulate genes involved in auxin synthesis and metabolism, transport, and signaling to affect root growth (Sun et al., 2010). *OsIAA11* was shown to inhibit LR growth (Jing et al., 2015) and *OsIAA13* positively regulated LR growth in rice (Kitomi et al., 2012). Thus, the active form, OsBZR1, is not phosphorylated by OsGSK2; this form induces the expression of *OsIAA13* and represses the expression of *OsIAA11*, leading to the overall LR formation. The transcriptomics microarray data on root cells in rice showed that OsHDAC1, OsGSK2, and OsBZR1 are co-expressed in roots (Takehisa et al., 2012). Taken together, the OsHDAC1–GSK2/OsBZR1 module controls LR formation in rice (Figure 7, E–H). Further investigations are required to determine how BL signaling components interplay with auxin-related genes to synergistically regulate LR formation in plants, which histone acetylases regulate OsGSK2 acetylation, and how the phosphorylation and acetylation of OsGSK2 are synergistically regulated.

Materials and methods

Plant materials and growth conditions

Wild-type rice of Nipponbare and mutant seeds in the Nipponbare background were soaked in 75% (v/v) ethanol for 1 min and then in 15% (w/v) NaClO for 15 min. They were then washed five times in double-distilled water. Seeds were stratified in water for 24 h at 37°C in the dark; they were then transferred to Murashige and Skoog liquid medium under 16-h light/28°C and 8-h dark/26°C, 70% relative humidity for 5 d. *Nicotiana benthamiana* plants were grown at 20 ± 2°C, a photoperiod of 8 h, and in soil for 6 weeks.

Hormone and inhibitor treatments

BL (APEX BIO, USA), Bikinin (Selleck Chemicals, USA) and TSA (Selleck Chemicals) were dissolved in dimethyl sulfoxide. For hormone and inhibitor treatments, sterilized rice seeds were planted in Murashige and Skoog liquid medium containing the indicated concentration of BL, Bikinin, or TSA for 5 d. The control groups were grown in an identical volume of dimethyl sulfoxide as a mock treatment.

Root phenotyping analysis

Five-day-old rice seedlings were collected for phenotyping analysis; initial and emerging LR numbers were counted using a Leica microscope. The root system was scanned by a Nikon camera scanner and measured using Image J software.

Plasmid construction and generation of transgenic plants

For the purification of GST–OsHDAC1, OsGSK2–His, and MBP–OsBZR1 recombinant proteins, the *OsHDAC1* CDS

fragment was amplified and cloned into the pGEX4T-1 vector, the *OsGSK2* CDS fragment was inserted into the pET28a vector, and the full length *OsBZR1* CDS fragment was inserted into the pMalC2x vector. To generate *OsHDAC1*-sGFP for subcellular localization, the *OsHDAC1* CDS fragment was cloned into the HBT-sGFP vector. To generate the *OsHDAC1*-BD, *OsGSK2*-AD, and *OsBZR1*-AD constructs for yeast two-hybrid assays, the *OsHDAC1* CDS fragment was amplified and cloned into the pGBKT7 vector, while the *OsGSK2* and *OsBZR1* CDS fragments were PCR-amplified and cloned into the pGADT7 vector. To generate the pBridge-*OsBZR1*-*OsHDAC1* constructs for yeast three-hybrid assays, the *OsBZR1* CDS fragments were PCR-amplified and inserted into the multiple cloning site (MCS) I sites of the pBridge vector; the *OsHDAC1* CDS fragments were PCR-amplified and inserted into the MCS II sites of pBridge-*OsBZR1* constructs. To generate the *OsHDAC1*-nLUC and cLUC-*OsGSK2* constructs, the *OsHDAC1* CDS fragments were cloned into the pCambia1300-nLUC vector, while *OsGSK2* CDS fragments were cloned into the pCambia1300-cLUC vector.

To generate *OsHDAC1* RNA interference plants, the *OsHDAC1*-RNAi vector was constructed by sequentially inserting two inverted copies of a 202-base pair-specific cDNA fragment of *OsHDAC1* (nucleotides 355–556) into the pCambia1300 vector. To generate *OsGSK2* mutant plants, two sgRNAs for the CRISPR/Cas9 system and plasmid construction were designed as described previously (Ma et al., 2016). CRISPR-P (<http://cbi.hzau.edu.cn/crispr>) was used to select sgRNAs targeting exons of genes of interest. The Cas9 destination vector was driven by the maize ubiquitin promoter for expression in rice; sgRNA expression was driven by the pol III type promoter of U6 sgRNA. The Gibson Assembly Cloning method was used to ligate the sgRNA to the Cas9 destination vector; Cas9 and the sgRNA were inserted into the pCambia1300 binary T-DNA vector. To generate *OsHDAC1*, *OsGSK2*, and *OsBZR1* overexpression plants, the *OsHDAC1* CDS fragments were fused to a HA tag, *OsGSK2* CDS fragments were fused to a MYC tag, and *OsBZR1* CDS fragments were fused to a FLAG tag to generate fusion genes; all fusion genes were cloned into a pCXUN vector. These vectors were transformed by *Agrobacterium tumefaciens* (strain EHA105)-mediated infection into wild-type plants to generate *OsHDAC1*-, *OsGSK2*-, and *OsBZR1*-overexpressing lines. T2 seedlings of these transgenic lines were used for the phenotypic evaluation.

RNA extraction and RT-qPCR

RT-qPCR analysis of gene expression was performed as described by Hou et al. (2021). Total RNA was extracted from rice organs using Trizol reagent (Invitrogen, USA); purified RNA was reverse-transcribed to cDNA using the Revert Aid First-Strand cDNA Synthesis Kit (Fermentas, Canada). Synergy Brands Green Real-Time PCR Master Mix (TOYOBO, Japan) was used to perform RT-qPCR on a StepOne Plus Real-Time PCR system. The rice *GAPDH* gene

was used as an internal control (Hou et al., 2021). The $2^{-\Delta\Delta Ct}$ method was used to calculate relative mRNA levels.

Subcellular localization assay

To evaluate the subcellular localization of *OsHDAC1*, *OsHDAC1*-sGFP constructs were transformed into rice protoplasts as described previously (Hu et al., 2013). The transformed protoplasts were photographed using a confocal laser-scanning microscope (Leica SP8, USA; i.e. lasers, intensity, collection bandwidth, and gains) used for the confocal work.

Images were analyzed with Image LAS-AF software.

The settings used for confocal microscopy were as follows (in nm: excitation [ex] and emission [em]): for sGFP, ex 488, em 500–550; for RFP, ex 552, em 575–625; fluorescence intensity, 5%; gains value, 500–800.

Phylogenetic analysis

The full-length protein sequences of *OsHDAC1* homologs in rice and Arabidopsis were used to construct a phylogenetic tree by the neighbor-joining method in MEGA 7.0. The parameters were as follows: complete deletion and 1,000 bootstrap replicates.

Methylene blue staining

Methylene blue staining was performed to detect rice LRP. Root samples were incubated in FAA solution (18:1:1 {v/v/v} 70% alcohol: acetic acid: formalin) at 4°C for 24 h. After samples had been washed three times in ddH₂O for 10 min each, they were transferred to 0.01% (w/v) methylene blue solution for 5 min, and then washed with ddH₂O for 10 min. A Nikon SMZ25 stereomicroscope was used to obtain images of the LRPs.

Protein extraction and immunoblotting

For protein extraction, fresh samples were ground to powder with liquid nitrogen and resuspended in protein extraction buffer (100-mM Tris-HCl, pH 7.4, 50-mM NaCl, 5-mM ethylenediaminetetraacetic acid, 1× cocktail [Roche], and 1-mM phenylmethylsulfonyl fluoride). Samples were heated for 10 min at 100°C, and then centrifuged at 13,000g for 10 min at room temperature. The supernatants were transferred into new tubes; total protein concentrations were measured by the Bradford method, in accordance with the manufacturer's instructions (Bio-Rad Protein Assay, USA). For immunoblotting, proteins were separated by electrophoresis in a 12% sodium dodecyl sulfate-polyacrylamide gel electrophoresis (SDS-PAGE) gel, transferred to polyvinylidene fluoride membranes, and immunoblotted as described previously (Hou et al. 2017). For Coomassie brilliant blue (CBB) gel staining, proteins were separated by electrophoresis in a 12% SDS-PAGE gel and then stained by using CBB fast staining solution (Cat#PA101-01, TIANGEN, China) according to the manufacturer instruction.

The antibodies used were anti-*OsGSK2* (Cat#AbP80050-A-SE, Beijing Protein Innovation, China, 1:1000), anti-*OsBZR1* (Cat#AbP80051-A-SE, Beijing Protein Innovation,

1:1000), anti-Actin (Cat#E021111-01, EarthOx, USA, 1:1000 dilution), anti-HA (Cat#51064-2-AP, Proteintech, China, 1:2000), anti-MYC (Cat#60003-2-Ig, Proteintech, 1:2000), anti-FLAG (Cat#20543-1-AP, Proteintech, 1:2000), anti-GST (Cat#66001-2-Ig, Proteintech, 1:2000), anti-His (Cat#66005-1-Ig, Proteintech, 1:2000), anti-MBP (Cat#66003-1-Ig, Proteintech, 1:2000), and anti-LysAc (Cat#3067, Dia-an, China, 1:2000).

Yeast screening assay and yeast two-hybrid assay

For yeast screening assay, Full-length OsHDAC1 was cloned into the pGBKT7 vector using the Matchmaker GAL4 Two-Hybrid System 3, in accordance with the manufacturer's instructions (Clontech, USA), and then the construct was transformed into the yeast strain Y2HGold. The transformed Y2HGold yeast strain was fused with the Y187 yeast strain containing a rice cDNA library constructed in the pGADT7 vector. The medium lacking Leu–Trp–His–Ade was used for selection. Positive clones were selected for sequencing.

The interactions between OsHDAC1 and OsGSK2 were verified by yeast two-hybrid assays according to the Matchmaker GAL4 Two-Hybrid System 3 manufacturer's manual (Clontech, USA). The prey plasmid, pGADT7-OsGSK2 or pGADT7-OsBZR1, was co-transformed with the bait plasmid, pGBKT7-OsHDAC1 into *Saccharomyces cerevisiae* strain AH109. After transformants had been cultured on synthetic medium plates (SD medium) lacking Trp and Leu (SD/–Trp/–Leu) at 30°C for 2 d, they were transferred onto medium plates (SD/–Trp–Leu–His–Ade) for development.

Split luciferase complementation assay

For split luciferase complementation assays, *Agrobacterium* GV3101 cells containing cLUC-OsGSK2 and OsHDAC1-nLUC vector pairs were transformed into *N. benthamiana* leaves, as described elsewhere (Li et al., 2020). *N. benthamiana* leaves were sprayed with 0.5-mM luciferin and incubated in the NightOWL II LB983 imaging apparatus for 5 min before luminescence detection.

Yeast three-hybrid assay

Yeast three-hybrid analysis was performed as described previously (Zhang et al., 2017). Constructs expressing OsBZR1 and bridge protein OsHDAC1 or expressing OsBZR1 were generated. *Saccharomyces cerevisiae* strain AH109 was transformed with a pair of plasmids, pBridge–OsBZR1–OsHDAC1 and pGADT7–OsGSK2, or with pBridge–OsBZR1 and pGADT7–OsGSK2. pBridge and pGADT7–OsBZR1 or pBridge–OsBZR1 and pGADT7 were used as the negative control. The transformed colonies were screened on synthetic medium (SD/–Leu/–Met/–Trp) and the transformants were transferred onto plates (SD/–Ade/–Met/–Trp/–Leu/–His) for development.

Coimmunoprecipitation assays

To verify the in vivo interaction between OsHDAC1 and OsGSK2, coimmunoprecipitation assays were performed as described previously (Zhang et al., 2017). Total proteins

were extracted from rice protoplasts expressing two pairs of plasmids (OsHDAC1-HA and OsGSK2-MYC or HA and OsGSK2-MYC) and incubated with rProtein A sepharose (GE Healthcare, USA) and an anti-HA antibody. Proteins bound to sepharose were detected using an anti-MYC antibody.

For the interference assay, proteins were extracted from rice protoplasts expressing OsGSK2-MYC and OsBZR1-Flag with or without OsHDAC1-HA. Anti-MYC-rProtein A sepharose was used to purify the protein complex. After separation and blotting, protein bands were detected using an anti-Flag antibody.

In vitro purification of recombinant proteins

GST-HDAC1, OsGSK2-His, and MBP-OsBZR1 proteins were purified as described previously (Ye et al., 2019). These constructs were transferred into *E. coli* strain BL21DE3; expression was induced by adding 0.5-mM isopropyl β -D-1-thiogalactopyranoside to the culture for 12 h at 16°C. The fusion proteins were purified by affinity chromatography.

In vitro pull-down assays

In vitro pull-down assays were performed by incubating GST or OsHDAC1-GST coupled GST-tag purification resin (Beyotime, China) with OsGSK2-His for 2 h at 4°C; the complexes were washed thoroughly, boiled in SDS–PAGE sample buffer for 10 min, and analyzed by immunoblotting using an anti-His antibody.

For the in vitro interference assays, purified OsGSK2-His and MBP-OsBZR1 were incubated with or without GST-OsHDAC1 in deacetylase buffer (50-mM Tris, pH 8.0, 137-mM NaCl, 2.7-mM KCl, 1-mM MgCl₂, 1- μ M ZnCl₂, and 1-mM dithiothreitol) at 37°C for 3 h, as described previously with minor modification (Xu et al., 2021). Next, the reactions were stopped by adding stop buffer (1-M HCl and 0.16-M acetic acid). Subsequently, His-tag purification resin was used to purify the protein complex. After separation and blotting, protein bands were detected using an anti-MBP antibody.

OsHDAC1 activity assay in vitro

To assay the deacetylation activity of OsHDAC1, a suitable amount of purified GST-OsHDAC1 was used to test in vitro HDAC activity using an HDAC Activity/Inhibition Direct Assay Kit (Cat#P-4034, Epigentek, USA), in accordance with the manufacturer's instructions. After the reactions were complete, the absorbance at 450 nm was measured using a microplate reader.

In vivo and in vitro OsGSK2 acetylation and activity assays

In vitro deacetylation assays were performed as described previously with modifications (Xu et al., 2021). Briefly, total proteins from OsGSK2 OE5 plants were extracted using a Protein Extraction Kit (Cat#319815, BestBio, China), in accordance with the manufacturer's instructions, then incubated with an rProtein A sepharose-coated anti-OsGSK2 antibody

for 12 h at 4°C. Finally, OsGSK2-MYC protein purified from plants or OsGSK2-His from *E. coli* was incubated with or without GST-OsHDAC1 in deacetylase buffer at 37°C for 3 h. The products were subjected to immunoblotting analysis using an anti-LysAc antibody. For *in vivo* OsGSK2 deacetylation assays, 5-d-old roots of wild-type, *OsHDAC1* Ri2, Ri3, OE5, and OE6 plants were collected. Samples were ground into powder with liquid nitrogen and extracted using a Protein Extraction Kit (Cat#319815, BestBio, China), then incubated with an rProtein A sepharose-coated anti-OsGSK2 antibody for 12 h at 4°C. After three washes with phosphate-buffered saline plus Tween, the coimmunoprecipitated proteins were separated by SDS-PAGE and detected using anti-GSK2 and anti-LysAc antibodies. *In vivo*- and *in vitro*-acetylated OsGSK2 protein was subjected to kinase activity assays using the plant GSK3/SHAGGY-like kinases assay system (MLBio, China), in accordance with the manufacturer's instructions. After the reactions were complete, the absorbance at 450 nm was measured using a microplate reader.

Statistical analysis

Student's *t* test (*t* test) was used to perform comparisons of two groups in Excel software (2018). All *P*-values were two-tailed. "Type 2" was chosen for equivariance hypothesis between two groups. Values of *P* < 0.05 were considered to indicate statistical significance.

Primer sequences

The sequences of primers used in this study are listed in [Supplementary Table S1](#).

Accession numbers

Sequence data from this article can be found in the GenBank/NCBI libraries under the following accession numbers: *OsHDAC1* (AF513382), *OsHDAC2* (AF513383), *OsHDAC3* (AF513384), *OsGSK2* (AK102147), *OsBZR1* (AK106748), *OsIAA11* (Q0DQ61), and *OsIAA13* (AK059838).

Supplemental data

The following materials are available in the online version of this article.

Supplemental Figure S1. eFP browser view of the expression pattern of *OsHDAC1*.

Supplemental Figure S2. Alignment of the Class I RPD3-type HDAC subfamily in rice and Arabidopsis.

Supplemental Figure S3. Subcellular localization analysis of OsHDAC1 in rice protoplasts.

Supplemental Figure S4. Diagrammatic representation of the vector constructs and expression analysis of *OsHDAC1* in transgenic plants.

Supplemental Figure S5. Induction and purification of proteins used for pull-down, immunoblot, and kinase activity analysis.

Supplemental Figure S6. Diagrammatic representation of the vector constructs and expression analysis of *OsGSK2* in transgenic plants.

Supplemental Figure S7. Phenotype identification of rice roots after BL treatment.

Supplemental Figure S8. Diagrammatic representation of the vector constructs and expression analysis of *OsBZR1* in transgenic plants.

Supplemental Figure S9. OsHDAC1 does not interact with OsBZR1.

Supplemental Table S1. Primers used for plasmid construction, transgene plant identification, and RT-qPCR in this study.

Acknowledgments

We are grateful for support from staff of the State Key Laboratory of Hybrid Rice (Wuhan University). We thank the editor and reviewers for critically evaluating the manuscript and providing constructive comments for its improvement.

Funding

This work was supported by National Natural Science Foundation of China (NSFC No. 31871238 and No.31801026).

Conflict of interest statement. The authors declare that they have no conflicts of interest.

References

- Bao F, Shen J, Brady SR, Muday GK, Yang AZ (2004) Brassinosteroids interact with auxin to promote lateral root development in Arabidopsis. *Plant Physiol* **134**: 1624–1631
- Bhalerao RP, Eklof J, Ljung K, Marchant A, Bennett M, Sandberg G (2002) Shoot-derived auxin is essential for early lateral root emergence in Arabidopsis seedlings. *Plant J* **29**: 325–332
- Chen X, Ding AB, Zhong X (2020) Functions and mechanisms of plant histone deacetylases. *Sci China Life Sci* **63**: 206–216
- Chung PJ, Kim YS, Jeong JS, Park SY, Nahm BH, Kim JO (2009) The histone deacetylase OsHDAC1 epigenetically regulates the OsNAC6 gene that controls seedling root growth in rice. *Plant J* **59**: 764–776
- Coudert Y, Périn C, Courtois B, Khong NG, Gantet P (2010) Genetic control of root development in rice, the model cereal. *Trends Plant Sci* **15**: 219–226
- Ding B, Bellizzi MDR, Ning Y, Meyers BC, Wang GL (2012) HDT701, a histone H4 deacetylase, negatively regulates plant innate immunity by modulating histone H4 acetylation of defense-related genes in rice. *Plant Cell* **24**: 3783–3794
- Dubrovsky JG, Doerner PW, Colon-Carmona A, Rost TL (2000) Pericycle cell proliferation and lateral root initiation in Arabidopsis. *Plant Physiol* **124**: 1648–1657
- Fukaki H, Tasaka M (2009) Hormone interactions during lateral root formation. *Plant Mol Biol* **69**: 437–449
- Gifford ML, Banta JA, Katari MS, Hulsmans J, Chen L, Ristova D, Tranchina D, Purugganan MD, Coruzzi GM, Birnbaum KD (2013) Plasticity regulators modulate specific root traits in discrete nitrogen environments. *PLoS Genet* **9**: e1003760
- Hao Y, Wang H, Qiao S, Leng L, Wang X (2016) Histone deacetylase HDA6 enhances brassinosteroid signaling by inhibiting the BIN2 kinase. *Proc Natl Acad Sci USA* **113**: 10418–10423 [PMC][10.1073/pnas.1521363113] [27562168]
- Hou H, Zheng X, Zhang H, Yue M, Hu Y, Zhou H, Wang Q, Xie C, Wang P, Li L (2017) Histone deacetylase is required for

- GA-induced programmed cell death in maize aleurone layers. *Plant Physiol* **175**: 1484–1496
- Hou J, Ren R, Xiao H, Chen Z, Yu J, Zhang H, Shi Q, Hou H, He S, Li L** (2021) Characteristic and evolution of HAT and HDAC genes in Gramineae genomes and their expression analysis under diverse stress in *Oryza sativa*. *Planta* **253**: 72
- Hu J, Huang W, Huang Q, Qin X, Dan Z, Yao G, Zhu R, Zhu Y** (2013) The mechanism of *ORFH79* suppression with the artificial restorer fertility gene *Mt-GRP162*. *New Phytol* **199**: 52–58
- Jia Z, Giehl RFH, von Wirén N** (2021) Local auxin biosynthesis acts downstream of brassinosteroids to trigger root foraging for nitrogen. *Nat Commun* **12**: 5437
- Jing H, Yang X, Zhang J, Liu X, Zheng H, Dong G, Nian J, Feng J, Xia B, Qian Q, et al.** (2015) Peptidyl-prolyl isomerization targets rice Aux/IAAs for proteasomal degradation during auxin signalling. *Nat Commun* **6**: 7395
- Jang IC, Pakk YM, Sang IS, Kwon HJ, Nahm BH** (2003) Structure and expression of the rice class-I type histone deacetylase genes *OsHDAC1-3*: *OsHDAC1* overexpression in transgenic plants leads to increased growth rate and altered architecture. *Plant J* **33**: 531–541
- Kim TW, Guan S, Sun Y, Deng Z, Tang W, Shang JX, Sun Y, Burlingame AL, Wang ZY** (2009) Brassinosteroid signal transduction from cell-surface receptor kinases to nuclear transcription factors. *Nat Cell Biol* **11**: 1254–1260
- Kitomi Y, Inahashi H, Takehisa H, Sato Y, Inukai Y** (2012) *OsIAA13*-mediated auxin signaling is involved in lateral root initiation in rice. *Plant Sci* **190**: 116–122
- Li J, Terzaghi W, Gong Y, Li C, Ling JJ, Fan Y, Qin N, Gong X, Zhu D, Deng XW** (2020) Modulation of BIN2 kinase activity by HYS controls hypocotyl elongation in the light. *Nat Commun* **11**: 1592
- Lv B, Wei K, Hu K, Tian T, Zhang F, Yu Z, Zhang D, Su Y, Sang Y, Zhang X, et al.** (2021) MPK14-mediated auxin signaling controls lateral root development via ERF13-regulated very-long-chain fatty acid biosynthesis. *Mol Plant* **14**: 285–297
- Ma X, Zhu Q, Chen Y, Liu YG** (2016) CRISPR/Cas9 platforms for genome editing in plants: developments and applications. *Mol Plant* **9**: 961–974
- Malamy JE** (2005) Intrinsic and environmental response pathways that regulate root system architecture. *Plant Cell Environ* **28**: 67–77
- Mao C, He J, Liu L, Deng Q, Yao X, Liu C, Qiao Y, Li P, Ming F** (2020) *OsNAC2* integrates auxin and cytokinin pathways to modulate rice root development. *Plant Biotechnol J* **18**: 429–442
- Marhavý P, Montesinos JC, Abuzeineh A, Van Damme D, Vermeer JE, Duclercq J, Rakusová H, Nováková P, Friml J, Geldner N, et al.** (2016). Targeted cell elimination reveals an auxin-guided biphasic mode of lateral root initiation. *Genes Dev* **30**: 471–483
- Meng F, Xiang D, Zhu J, Li Y, Mao C** (2019) Molecular mechanisms of root development in rice. *Rice* **12**: 1
- Motte H, Vanneste S, Beekman T** (2019) Molecular and environmental regulation of root development. *Annu Rev Plant Biol* **70**: 465–488
- Narita T, Weinert BT, Choudhary C** (2019) Functions and mechanisms of non-histone protein acetylation. *Nat Rev Mol Cell Biol* **20**: 156–174
- Orman-Ligeza B, Parizot B, Gantet PP, Beekman T, Bennett MJ, Draye X** (2013) Post-embryonic root organogenesis in cereals: branching out from model plants. *Trends Plant Sci* **18**: 459–467
- Pandey R, Muller A, Napoli CA, Selinger DA, Pikaard CS, Richards EJ, Bender J, Mount DW, Jorgensen RA** (2002) Analysis of histone acetyltransferase and histone deacetylase families of *Arabidopsis thaliana* suggests functional diversification of chromatin modification among multicellular eukaryotes. *Nucleic Acids Res* **30**: 5036–5055
- Peng P, Yan Z, Zhu Y, Li J** (2008) Regulation of the Arabidopsis GSK3-like kinase BRASSINOSTEROID-INSENSITIVE 2 through proteasome-mediated protein degradation. *Mol Plant* **1**: 338–346
- Qiao S, Sun S, Wang L, Wu Z, Li C, Li X, Wang T, Leng L, Tian W, Lu T, et al.** (2017) The RLA1/SMOS1 transcription factor functions with OsBZR1 to regulate brassinosteroid signaling and rice architecture. *Plant Cell* **29**: 292–309
- Rogers ED, Benfey PN** (2015) Regulation of plant root system architecture: implications for crop advancement. *Curr Opin Biotechnol* **32**: 93–98
- Rossi V, Locatelli S, Varotto S, Donn G, Pirona R, Henderson DA, Hartings H, Motto M** (2007) Maize histone deacetylase *hda101* is involved in plant development, gene transcription, and sequence-specific modulation of histone modification of genes and repeats. *Plant Cell* **19**: 1145–1162
- Shen Y, Wei W, Zhou D** (2015) Histone acetylation enzymes coordinate metabolism and gene expression. *Trends in Plant Sci* **10**: 614–621
- Singh S, Yadav S, Singh A, Mahima M, Singh A, Gautam V, Sarkar AK** (2020) Auxin signaling modulates *LATERAL ROOT PRIMORDIUM1 (LRP1)* expression during lateral root development in Arabidopsis. *Plant J* **101**: 87–100
- Sun Y, Fan XY, Cao DM, Tang W, He K, Zhu JY, He JX, Bai MY, Zhu S, Oh E, et al.** (2010). Integration of brassinosteroid signal transduction with the transcription network for plant growth regulation in Arabidopsis. *Dev Cell* **19**: 765–777
- Takehisa H, Sato Y, Igarashi M, Abiko T, Antonio BA, Kamatsuki K, Minami H, Namiki N, Inukai Y, Nakazono M, et al.** (2012). Genome-wide transcriptome dissection of the rice root system: implications for developmental and physiological functions. *Plant J* **69**: 126–140
- Tanaka M, Kikuchi A, Kamada H** (2008) The Arabidopsis histone deacetylases HDA6 and HDA19 contribute to the repression of embryonic properties after germination. *Plant Physiol* **146**: 149–161
- To TK, Kim JM, Matsui A, Kurihara Y, Morosawa T, Ishida J, Tanaka M, Endo T, Kakutani T, Toyoda T, et al.** (2011). Arabidopsis HDA6 regulates locus-directed heterochromatin silencing in cooperation with MET1. *PLoS Genet* **7**: e1002055
- Tong H, Liu L, Jin Y, Du L, Yin Y, Qian Q, Zhu L, Chu C** (2012) DWARF AND LOW-TILLERING acts as a direct downstream target of a GSK3/ SHAGGY-like kinase to mediate brassinosteroid responses in rice. *Plant Cell* **24**: 2562–2577
- Wu K, Tian L, Zhou C, Brown D, Miki B** (2010) Repression of gene expression by Arabidopsis HD2 histone deacetylases. *Plant J* **34**: 241–247
- Wu X, Oh M-H, Schwarz EM, Larue CT, Sivaguru M, Imai BS, Yau PM, Ort DR, Huber SC** (2011) Lysine acetylation is a widespread protein modification for diverse proteins in Arabidopsis. *Plant Physiol* **4**: 1769–1778
- Xu P, Fang S, Chen H, Cai W** (2020) The brassinosteroid-responsive *xyloglucan endotransglucosylase/hydrolase 19 (XTH19)* and *XTH23* genes are involved in lateral root development under salt stress in Arabidopsis. *Plant J* **104**: 59–75
- Xu Q, Liu Q, Chen Z, Yue Y, Liu Y, Zhao Y, Zhou DX** (2021) Histone deacetylases control lysine acetylation of ribosomal proteins in rice. *Nucleic Acids Res* **49**: 4613–4628
- Ye K, Li H, Ding Y, Shi Y, Song C, Gong Z, Yang S** (2019) BRASSINOSTEROID-INSENSITIVE2 negatively regulates the stability of transcription factor ICE1 in response to cold stress in Arabidopsis. *Plant Cell* **31**: 2682–2696
- Youn J, Kim T** (2015) Functional insights of plant GSK3-like kinases: multi-taskers in diverse cellular signal transduction pathways. *Mol Plant* **8**: 552–565
- Yu P, Gutjahr C, Li C, Hochholdinger F** (2016) Genetic control of lateral root formation in cereals. *Trends Plant Sci* **21**: 951–961
- Yu P, Eggert K, von Wirén N, Li C, Hochholdinger F** (2015) Cell-type specific gene expression analyses by RNA-Seq reveal local high nitrate triggered lateral root initiation in shoot-borne roots of maize

- by modulating auxin-related cell cycle-regulation. *Plant Physiol* **169**: 690–704
- Yamauchi T, Tanaka A, Inahashi H, Nishizawa NK, Tsutsumi N, Inukai Y, Nakazono M** (2019) Fine control of aerenchyma and lateral root development through AUX/IAA- and ARF-dependent auxin signaling. *Proc Natl Acad Sci USA* **116**: 20770–20775
- Zhang Z, Li J, Li F, Liu H, Yang W, Chong K, Xu Y** (2017) OsMAPK3 phosphorylates OsbHLH002/OsICE1 and inhibits its ubiquitination to activate *OsTPP1* and enhances rice chilling tolerance. *Dev Cell* **43**: 731–743
- Zhao S, Xu W, Jiang W, Yu W, Lin Y, Zhang T, Yao J, Zhou L, Zeng Y, Li H, et al.** (2010). Regulation of cellular metabolism by protein lysine acetylation. *Science* **327**: 1000–1004
- Zhou C, Zhang L, Duan J, Miki B, Wu K** (2005) Histone deacetylase 19 is involved in jasmonic acid and ethylene signaling of pathogen response in *Arabidopsis*. *Plant Cell* **17**: 1196–1204